Magnetic and mineral fabric development in the Ordovician Martinsburg Formation in the Central Appalachian Fold and Thrust Belt, Pennsylvania

A. M. HIRT[1], W. LOWRIE[2], C. LÜNEBURG[3], H. LEBIT[3] & T. ENGELDER[4]

[1]*Institute of Geophysics, ETH-Hönggerberg, CH-8093 Zürich, Switzerland (e-mail: hirt@mag.ig.erdw.ethz.ch)*

[2]*Institute of Geophysics, ETH-Hönggerberg, CH-8093 Zürich, Switzerland*

[3]*Department. of Geology and Geophysics, University of New Orleans, New Orleans, LA 70148, USA*

[4]*Department of Geosciences, Pennsylvania State University, State College, PA 16802, USA*

Abstract: The Martinsburg Formation at Lehigh Gap, Pennsylvania, undergoes a transition from shales to slates, reflecting local progressive deformation on an outcrop scale. The anisotropy of magnetic susceptibility (AMS) was measured in low and high fields. The high-field measurements show that the magnetic susceptibility is controlled by the paramagnetic minerals. X-ray goniometry was used to define the mineral fabrics of chlorite and mica. The phyllosilicates are initially oriented preferentially in the bedding plane and are gradually reoriented into the cleavage plane through rotation, microfolding and recrystallization. The AMS fabric mirrors this change in mineral fabric. The magnetic fabric is originally oblate in the least deformed site, with the plane of flattening parallel to bedding, and becomes prolate with increasing deformation, reflecting the development of pencil structure in the shales. In the most deformed site, shortening results in a tectonic cleavage fabric, which controls the magnetic fabric. A similar pattern of fabric development can be observed on a regional scale at other sites across the central Appalachian fold and thrust belt. The AMS and mineral fabric from the Martinsburg Formation has undergone bedding compaction in the foreland near the Allegheny Front. The AMS and textural analysis both show that, as the deformation increases towards the hinterland, prolate fabrics develop and in the most deformed sites slaty cleavage controls both the mineral and magnetic fabrics.

The anisotropy of magnetic susceptibility (AMS) has been established as a qualitative proxy of petrofabrics since the mid-1950s. Graham (1954) demonstrated that the magnetic fabric reflects petrofabric, and Balsley & Buddington (1960) showed that magnetic methods were more sensitive in detecting fabrics than traditional microscopic methods. Several studies in the early 1960s further used magnetic anisotropy to determine petrofabrics and postulated on the origin of the magnetic fabric (e.g. Stacey *et al.* 1960; Girdler 1961; Fuller 1963). The authors were primarily interested in investigating whether a petrofabric could be responsible for a deviation of a rock's remanent magnetization. Graham (1966) pointed out that the magnetic susceptibility of a rock is composed of contributions from all constituent minerals in the rock, and that the magnetic anisotropy will depend on the orientations of crystal lattices or magnetite grain shapes. He examined the anisotropy of magnetic susceptibility (AMS) in flat-lying and folded Palaeozoic sediments from the Valley and Ridge Province of the Appalachian fold and thrust belt. The results from these studies led Graham (1966) to speculate on the development of a magnetic fabric during folding, where he considered the AMS to reflect the textural reorientation and grain rotation that occurs in the rock matrix during progressive deformation. The evolution of a magnetic fabric that undergoes horizontal compaction is continuous: it starts with an oblate ellipsoid that expresses flattening by the bedding compaction, and proceeds to a prolate ellipsoid with long axis parallel to the trend of the fold axis. Continued shortening leads to an oblate ellipsoid that is flattened in the cleavage plane and which can show extension down-dip in the cleavage plane at the highest stage of deformation.

X-ray texture goniometry provides information about the orientation of individual mineral phases in a rock. Ihmlé *et al.* (1989) were able to show in deformed limestones from the Morcles nappe in Switzerland that the principal axes of the AMS ellipsoid are related to the orientation of the crystallographic axes of calcite crystals. Hirt *et al.* (1995) demonstrated that a magnetic

From: MARTÍN-HERNÁNDEZ, F., LÜNEBURG, C. M., AUBOURG, C. & JACKSON, M. (eds) 2004. *Magnetic Fabric: Methods and Applications*. Geological Society, London, Special Publications, **238**, 109–126. 0305-8719/04/ $15.00

lineation in Devonian shales from the Allegheny Plateau was sub-parallel to the orientation of the long axes of chlorite crystals. Siegesmund *et al.* (1995) modelled the AMS of gneissic rocks from the mica texture. They found a good agreement in the orientation of the modelled and measured magnetic fabric, but a poor agreement of shape and degree of anisotropy. Since these first studies, there has been increasing interest in how magnetic fabrics reflect mineral fabrics (e.g. Lüneburg *et al.* 1999; Becker *et al.* 2000; de Wall *et al.* 2000).

This study returns to the area covered in Graham's (1966) seminal study in the Valley and Ridge Province of the Central Appalachian fold-thrust belt, to examine the development of mineral and magnetic fabrics in shales on two different spatial scales. Special attention was given to determining the minerals responsible for the AMS so that it could be compared with representative mineral fabrics. A detailed investigation of fabric development was made at Lehigh Gap on the hinterland edge of the Valley and Ridge in eastern Pennsylvania where, over the space of an outcrop, the Martinsburg Formation (locally called the Reedsville Formation) is progressively deformed from shale to slate. To establish whether the results from Lehigh Gap can be extended on a larger scale, the development of mineral and magnetic fabrics in the Martinsburg Formation was studied at four locations distributed across the Valley and Ridge of Pennsylvania. Magnetic anisotropy results were obtained from 33 additional sites in the Valley and Ridge. Because of the time-intensive nature of acquiring texture goniometry data, we selected four locations exhibiting different degrees of progressive deformation for detailed mineral fabric analysis.

Geological setting

The Central Appalachian Valley and Ridge Province has been extensively studied since H. D. & W. B. Rogers made the first structural geology maps in 1838–1846. It was an important area in developing the idea of thin-skinned tectonics (Rodgers 1963; Gwinn 1964). As recognized by Graham (1966), deformation in the Valley and Ridge follows two fundamental steps. The first step is a layer-parallel shortening (LPS), which is accommodated by pressure solution and other low-temperature creep mechanisms (e.g. Nickelsen 1966, 1979; Engelder & Geiser 1979; Geiser 1989; Geiser & Engelder 1983). On the Appalachian Plateau where LPS precedes major fold growth, stretch (S_3) by LPS is about 0.85 (Engelder & Engelder 1977). The second step is growth of first-order folds that 'behaved as a generally coherent and passive plate' (Graham 1949). The outer folds of the Valley and Ridge exhibit an LPS-related S_3 of about 0.85 (Faill 1977). Only in the anthracite district of the eastern Valley and Ridge of Pennsylvania is the LPS more intense and even there it predates the growth of major anticlines (Nickelsen 1979).

The Valley and Ridge behaves as two distinct mechanical units (Hatcher *et al.* 1989). A Cambrian-Ordovician carbonate sheet stacks as a duplex under a roof thrust in the Ordovician Martinsburg Formation (Geiser 1988). Interestingly, the carbonate thrust sheets show very little evidence of LPS where the roof exhibits well developed tectonic stretch, S_3 (e.g., Ferrill & Dunne 1989). The Ordovician Martinsburg Formation was deposited in a deep foreland basin during the Taconic orogeny (Faill 1997). It consists of fine-grained dark grey shales with interlayered siltstones and sandstones. Depending on where the Martinsburg sat relative to the roof thrust, it may exhibit a well-developed LPS fabric. If the Martinsburg sat below the roof-thrust detachment it may have ridden passively on carbonate horses below and thus exhibit virtually no LPS fabric. Conodant colour alteration indicates that most Ordovician rocks in Pennsylvania were never heated above 250 °C, except in the hinterland where slaty cleavage is developed (Epstein *et al.* 1977). Here temperatures may have exceeded 300 °C.

The geological setting of Lehigh Gap has been discussed extensively in other studies (e.g. Epstein & Epstein 1969; Holeywell & Tullis 1975; Wright *et al.* 1979; Wright & Platt 1982; Wintsch *et al.* 1991; Ho *et al.* 1995). The outcrop consists of the upper member of the Martinsburg Formation, which is conformably overlain by the Silurian Shawangunk Formation, a massive sandstone unit (Fig. 1). The Martinsburg Formation has a penetrative cleavage in this area of the Appalachian Fold-Thrust Belt. However, at the Lehigh Gap outcrop, the slaty cleavage in the Martinsburg Formation dies out within 30–60 m of the contact with the Shawangunk sandstone. Epstein & Epstein (1969) suggested that the quartzitic sandstone acts as a pressure shadow against cleavage formation in the shales. The bedding orientation remains relatively constant with dip direction of 327–336° and dip of 41–43° along the 120 m of outcrop that was sampled (Fig. 1). The Martinsburg shales show only bedding structure within the first metre from the contact with the Shawangunk Formation. The first pencil structures are identifiable about 2 m from the contact and are

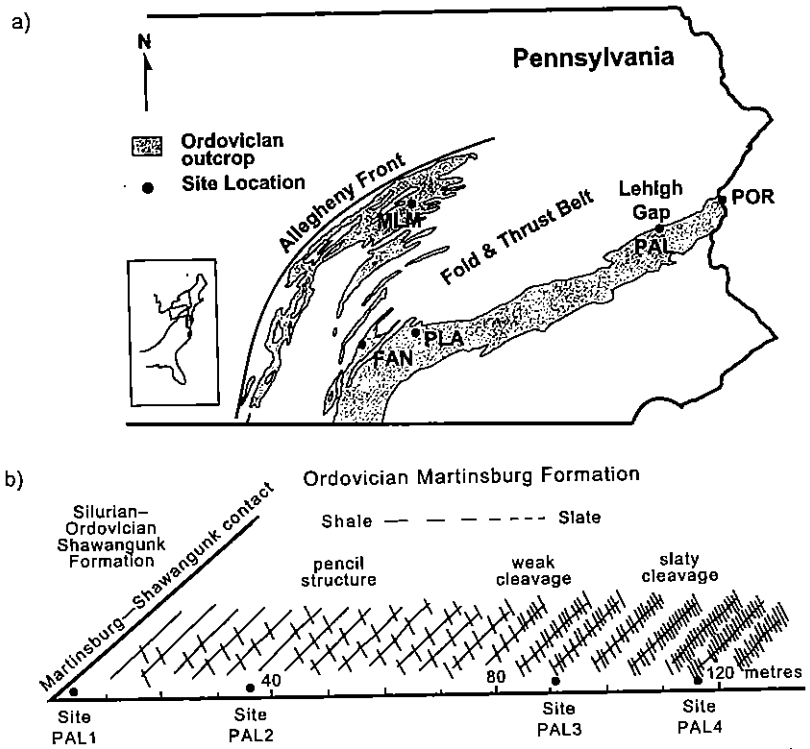

Fig. 1. (a) Map showing the sampling localities in the Appalachian fold and thrust belt and (b) schematic diagram of the Lehigh Gap outcrop in eastern Pennsylvania showing the stages of cleavage development and locations of the sampling sites relative to the contact with the Shawangunk sandstone (modified from Housen *et al.* 1995).

the dominant structure until the gradual appearance of cleavage between 60 and 80 m. The cleavage becomes stronger further along the outcrop where a penetrative slaty cleavage dominates. The cleavage plane has a dip direction of 171–186° and a dip of 56–59°. We sampled four sites along the 120 m outcrop at different distances from the contact: PAL1 within the first 3 m, PAL2 between 35 m and 40 m, PAL3 around approximately 90 m, and PAL 4 at around 120 m.

Four additional localities were selected across the Central Appalachian fold and thrust belt that represent progressive deformation from the foreland to the hinterland (Fig. 1). The sampling locations are named after the corresponding quadrangle of the geological map of Pennsylvania and are shown with related geological information in Table 1. MLM represents a region near the Allegheny Front in the foreland where only bedding compaction is observed. Samples were drilled in fine-grained siltstones from the SSW limb of the Nittany anticlinorium. Although pencil structures are found in fine-grained lithologies east of the Allegheny front, pervasive pencil structure occurs only in the area of FAN. Most samples at this locality came from siltier layers, since shaley units were too fractured to sample. The PLA outcrop covers a small asymmetric fold in which an incipient cleavage is visible in the more shaley units, and most samples were taken in shale and siltstone beds. A well-defined slaty cleavage is found in the hinterland at POR. The black slates show a strong lineation sub-parallel to the fold axis in the area.

Sampling and analytical techniques

Optical and electron microscopy methods

Microstructures of the shales and slates were studied by optical and electron microscopy in order to evaluate deformation mechanisms on the microscopic scale. Most studies were performed on a JEOL JSM 840 scanning electron microscope (SEM), which allows investigation of

Table 1. *Site locations and geological information*

Site	Location Quadrangle Lat/Long	Bedding Orientation Dip Direction/Dip	Cleavage Orientation Dip Direction/Dip	Lineation Dip/Dip Direction
LehighGap	Palmerton 40° 47′ N/77° 36′ W			
PAL1		328–335/42–43	*	07/252
PAL2		336–338/41–45	*	06/255
PAL3		325–333/36–42	170–173/48–54	11/256
PAL4		327/43	174–182/50–56	*
MLM	Millheim 40° 49′ N/77° 25.5′ W	167/42	*	*
FAN	Fannetsburg 40° 04.5′ N/77° 48.5′ W	149/33	*	02/58
PLA	Plainfield 40° 13′ N/77° 18′ W	150/70	152/70	*
POR	Portland 40° 54′ N/75° 04′ W	345/80	160/54	05/075

*Indicates none present

microstructures of very small grains, such as phyllosilicates, as well as their chemical compositions.

Two types of images were created: backscatter and secondary electron images. Backscatter images are performed on highly polished surfaces and reflect compositional differences since they are sensitive to the atomic number contrast. Secondary electron images are made from rough surfaces, treated with 48% hydrofluoric acid, and reflect the topographic relief of the grains. In addition Energy Dispersive X-ray Spectrometry (EDS) analysis allowed us to determine element spectra and quantitative analysis of sample areas or individual grains.

X-ray texture goniometry methods

For the X-ray texture goniometry measurements oriented block samples of 12 × 10 × 24 mm size were cut from adjacent parts of remaining cores from the magnetic fabric study. The measured surface was chosen as close as possible to the cleavage plane in order to obtain centred pole figures. The samples were analyzed with a Scintag-USA/DMS 2000 with a Cu X-ray source and a germanium solid-state detector, which measures the intensity of the K_α radiation directly. The mineral fabrics of mica and chlorite were determined by measuring the diffraction intensity of the dominant basal planes, (001) and (002) respectively, which determine the lattice as well as grain-shape preferred orientation (Oertel 1983; Siddans 1976). The data are illustrated in contoured pole figures in upper hemisphere projections, which represent scans of diffraction intensity in intervals of 5° (=1387 positions) (Casey 1981). In order to cover the full range of spherical orientations the samples are measured in reflection mode (as a block) and in transmission mode (as a thin section). The eigenvalues and eigenvectors of the intensity distributions determine shapes and principal axial orientations of fabric ellipsoids (e.g. Cheeney 1983; Davis 1986). The principal axes of the mineral fabric ellipsoids are described as $t_1 \geq t_2 \geq t_3$. The t_1 axis represents the largest eigenvector, which reflects the lowest intensity defined by the smallest number of poles to basal planes (c axes). The t_3 axis represents the smallest eigenvector, which reflects the highest intensity defined by the largest number of poles to basal planes (x axes). In the remainder of this text, t_1 is referred to as the maximum axis of the mineral fabric ellipsoid, t_2 as the intermediate axis and t_3 as the minimum axis. This convention is the same as used for describing the magnetic fabric axes. For comparison with magnetic directions the principal axes of the mineral fabrics were inverted and plotted on the lower hemisphere.

Magnetic methods

Eight cores, yielding nine to thirteen samples, were drilled with a portable gasoline drill at each locality at Lehigh Gap for the study of the magnetic fabric. Specimens had 2.54 cm diameter and 2.30 cm length. From 9 to 31 cores, yielding 18 to 54 specimens, were taken at each of the localities across the fold belt and prepared as above. The low-field anisotropy of magnetic

susceptibility (AMS) of all samples was measured with an AGICO KLY-2 susceptibility bridge (applied field: 0.4 mT, frequency: 920 Hz) at room temperature. Each sample was measured in 15 positions to obtain the susceptibility magnitude ellipsoid whose principal axes are $k_1 \geq k_2 \geq k_3$. Cooling the samples enhances the paramagnetic component of the susceptibility. Therefore, selected samples were measured at liquid nitrogen temperature (77 K), using the method outlined in Lüneburg *et al.* (1999).

In order to separate the paramagnetic or antiferrimagnetic component of the susceptibility anisotropy from the ferromagnetic component, the high-field anisotropy (HFA) of selected samples was measured on a torsion magnetometer, using the procedure described by Martín-Hernández & Hirt (2001). Samples were measured in four fields: 1200, 1400, 1600 and 1800 mT, all of which are above the saturation magnetization of the ferrimagnetic phases in the shales. The anisotropy of a partial anhysteretic remanent magnetization (ARM) was measured in two coercivity windows: 0–30 mT and 60–100 mT, in each case with a 0.1 mT d.c. bias field. We chose the low coercivity window so that we could compare our results with an earlier study of magnetic fabric at Lehigh Gap by Housen & van der Pluijm (1991). The ARM was imparted in 9 directions to over-define the anisotropy tensor and obtain an error estimate on the fit (McCabe *et al.* 1985), which was in the range 1–5%.

Magnetic mineralogy

The ferrimagnetic mineralogy was defined from (a) acquisition of anhysteretic remanent magnetization (ARM), (b) the acquisition of isothermal remanent magnetization (IRM) and (c) subsequent thermal demagnetization of a cross-component IRM. The ARM was acquired in a large coil in peak alternating fields up to 200 mT (Fig. 2a). The IRM was imparted with an electromagnet with a maximum field of 1.0 T (Fig. 2b). After magnetization in the 1.0 T field along the sample Z axis, a 0.5 T field was applied along the sample Y axis and a 0.1 T field along the sample X axis (Lowrie 1990). Samples were thermally demagnetized in a Schonstedt TSD-1 oven (Fig. 2c). Remanence was measured with a 2G 3-axis cryogenic magnetometer with RF SQUIDs.

The ARM acquisition curves are still rising steeply at 30 mT, but have reached most of their maximum intensity by 100 mT (Fig. 2a). The IRM acquisition curves of the shales and slates show a rapid increase in magnetization below 0.15 T, where they are close to saturation; the magnetization is saturated by 0.5 T (Fig. 2b). Thermal demagnetization of the cross-component IRM is similar in most samples (Fig. 2c). The magnetization is dominated by the low coercivity component, which is fully demagnetized by 600 °C. A more rapid loss in magnetization occurs between 500 and 600 °C and a less dramatic loss between 300 and 350 °C. The medium and high coercivity components undergo little unblocking until 300 °C where the intensity drops more rapidly. The remaining magnetization is generally unblocked by 600 °C. These results suggest that magnetite is the dominant ferrimagnetic phase in the Martinsburg Formation with a smaller contribution from pyrrhotite.

Lehigh Gap, Pennsylvania

Electron microscopy and texture goniometry

Electron microscopy at PAL1, the least deformed site, shows that the phyllosilicates, particularly the mica, are mainly oriented in the bedding plane, although some kinking can be observed (Fig. 3). Chlorite grains have been identified lying at an angle to the main bedding orientation, as also observed by Holeywell & Tullis (1975) and Ho *et al.* (1995). The mica and chlorite mineral fabrics show a distribution of the c axes in a weak girdle structure, whose pole t_1 is sub-parallel to the pencil structure lineation (Fig. 4). The average of the chlorite minimum axes t_3 is at an angle of about 30° to the bedding plane, whereas the mica average is close to the bedding pole. Both mineral fabrics reflect the microscopic observations.

Pencil structures are well developed at PAL2. The phyllosilicate minerals tend to lie flattened in the bedding or kinked at an angle to the bedding plane (Fig. 3). The mineral fabric is similar to PAL1; the main difference is that the average of the chlorite minimum axes now lies closer to the bedding plane pole (Fig. 4). The minimum axes of the mica and chlorite are well grouped around the pole to bedding and the maximum axes are still grouped about the visible intersection lineation.

At 90 m from the contact at PAL3 a slaty cleavage has developed and the intersection lineation is evident from the pencil structures. SEM studies show a stronger preferred orientation of the phyllosilicate grains and increased kinking (Fig. 3). The kinking is responsible for the more pronounced girdle structure of the

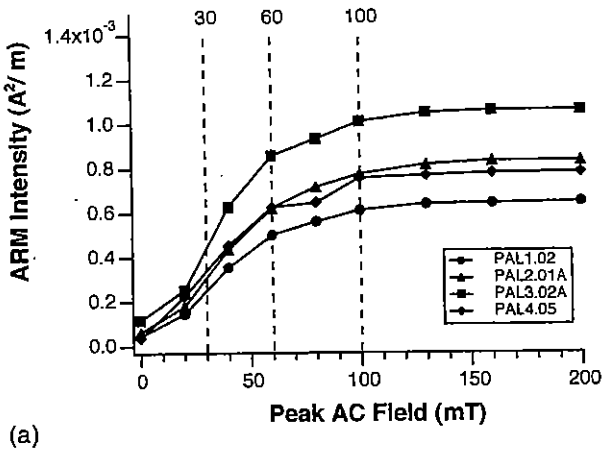

(a)

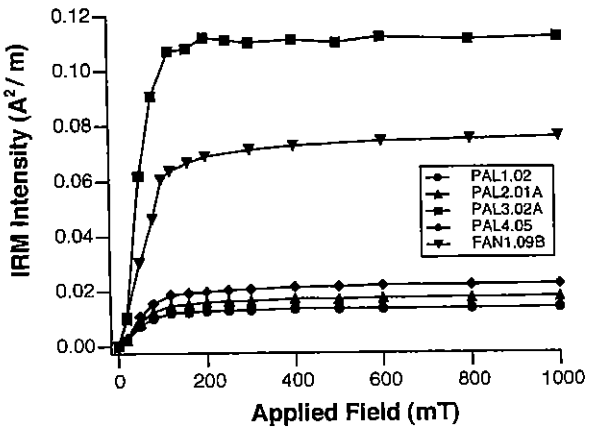

(b)

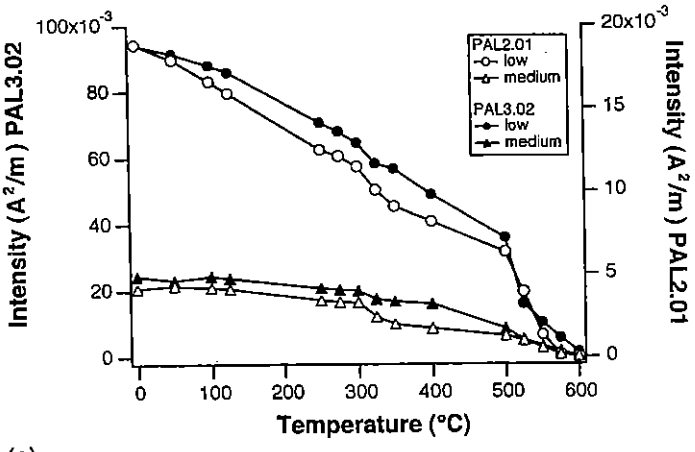

(c)

Fig. 2. (a) ARM acquisition and (b) IRM acquisition in representative samples from several Appalachian sites. (c) Thermal demagnetization of a cross-component IRM for two representative samples.

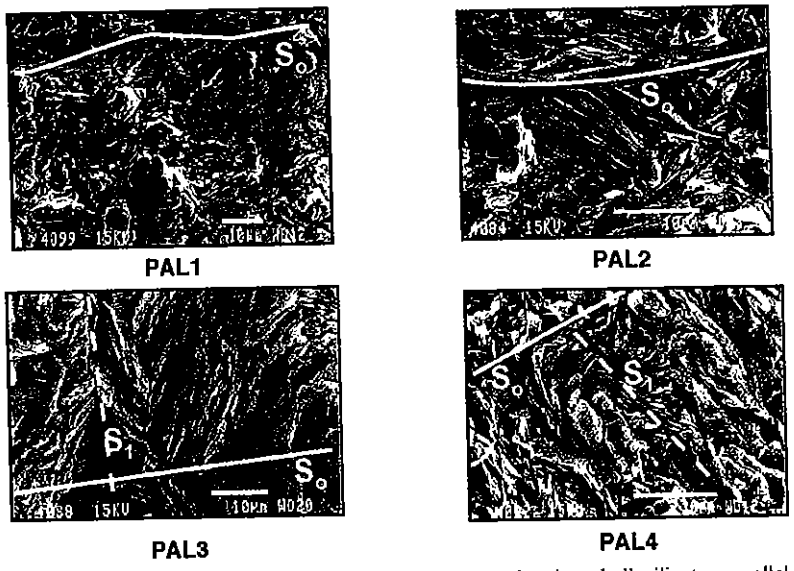

Fig. 3. SEM secondary electron images of the Lehigh Gap samples showing phyllosilicates parallel to bedding at PAL1 and increasing grain rotation, kinking and microfolding from PAL2 to PAL3 and PAL 4. Cleavage is defined by phyllosilicates parallel to the cleavage plane and the kink axial planes. Scale bar is 10 μm in each image. S_0 and S_1 are the traces of the bedding and cleavage planes, respectively.

mica fabric (Fig. 4). The chlorite fabric is very weak, and may be controlled by a few large crystals in the section. However, the minimum axes are close to the bedding pole. In contrast, the mica minimum axis lies between the bedding and the cleavage poles. The intersection lineation still controls the mineral fabrics.

A pervasive slaty cleavage is developed at PAL4. Grains still show kinking, but new growth of grains and grain rotation within the cleavage plane are also visible (Fig. 3), leading to a stronger alignment of the phyllosilicates with the macroscopic cleavage plane. The mineral fabric is still dominated by the intersection lineation. As at site PAL3 the mica maximum axes form a girdle structure about the intermediate axis whereas the chlorite maxima form a weak cluster.

Anisotropy of magnetic susceptibility in low and high fields

The magnetic fabric at room temperature shows that k_1 maximum axes are well-grouped about the lineation, similar to the phyllosilicate maximum axes (t_1), and k_3 minimum axes are offset from the pole to bedding, lying between the mica and chlorite minimum axes (t_3) (Figs 5 & 6). PAL2 shows a similar AMS fabric. The magnetic fabrics at PAL1 and PAL2 are similar to the magnetic fabric reported by Housen & van der Pluijm (1991). At site PAL3 the k_1 axes are tightly grouped about the intersection lineation and the k_2 and k_3 axes are distributed in a plane normal to the lineation. The k_3 axes from specimens of coarser-grained siltstone are oriented closer to the bedding pole, whereas specimens taken from finer-grained siltstones lie closer to the cleavage pole (Fig. 5). The magnetic fabric at PAL4 has k_3 axes normal to cleavage and k_1 axes grouped around a stretching lineation within the cleavage.

The AMS measured at liquid nitrogen temperature shows an increase over the room temperature values that average around 3.5 for all samples from Lehigh Gap. This is close to the ratio of 3.8, which would be expected if the AMS is controlled solely by paramagnetic minerals. The directions of the principal axes of the magnetic fabric at 77 K agree within a few degrees with those measured at room temperature and shown in Fig. 5.

High-field torque is linearly proportional to the squared field in all samples from Lehigh Gap, which indicates that only paramagnetic phases contribute to the susceptibility anisotropy. The principal axes of the paramagnetic component agree well with the low-field AMS measured at both room temperature and liquid nitrogen temperature, which further supports the assumption that only paramagnetic phases are responsible for the observed anisotropy (Fig. 6).

chian sites.

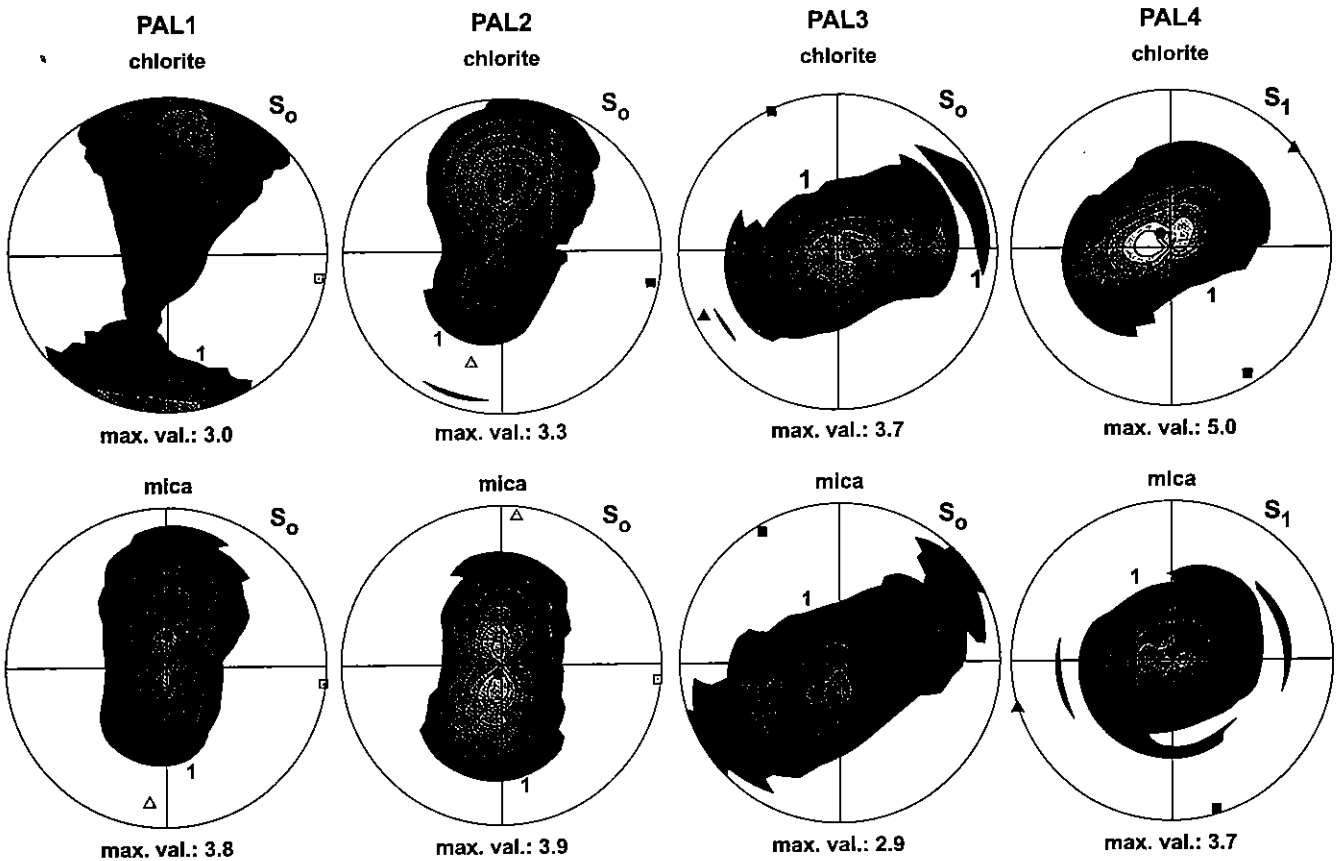

Fig. 4. X-ray texture goniometry pole figures of mica and chlorite for the Lehigh Gap samples. Contour interval is 0.5 m.r.d. (multiples of random distribution). With increasing deformation the mica fabric develops from a cluster to a girdle distribution. The chlorite fabric shows an angle to bedding and less pronounced girdle structures. The mean directions of t_1 axes are shown by squares, t_2 axes by triangles and t_3 axes by circles; S_0 and S_1 are the bedding and cleavage planes, respectively.

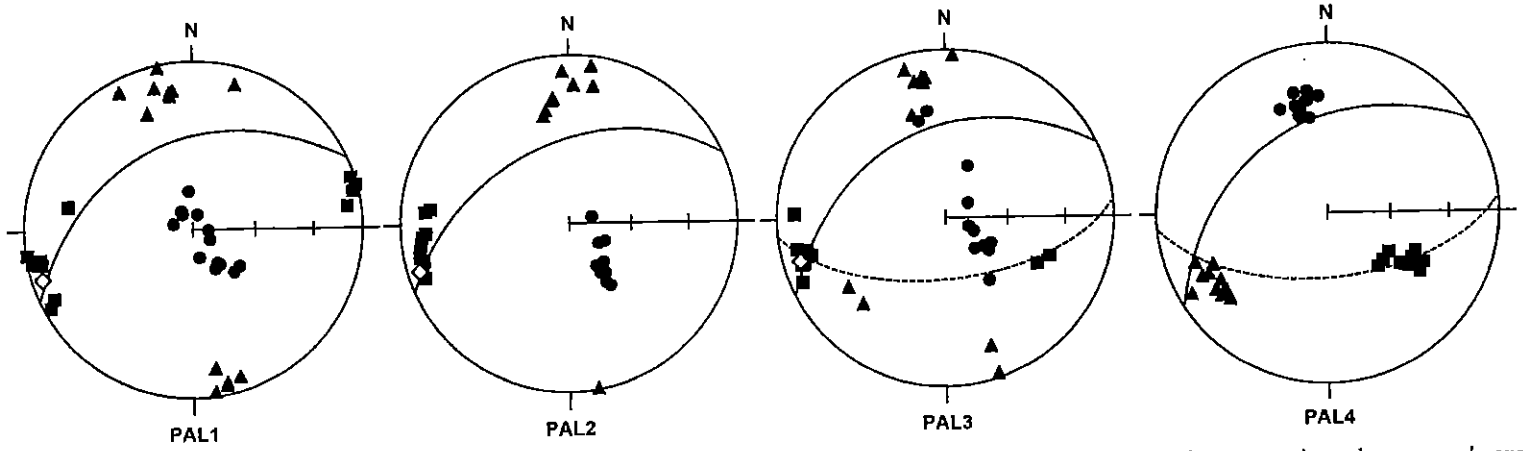

Fig. 5. Orientations of the principal axes of the low-field AMS ellipsoid in Lehigh Gap sites, measured at room temperature. The k_1 axes are shown by squares, k_2 axes by triangles and k_3 axes by circles. The bedding plane is shown with a solid line, cleavage plane with a dotted line, and pencil lineation with a white diamond in this and subsequent figures. Plots are lower-hemisphere, equal area projections.

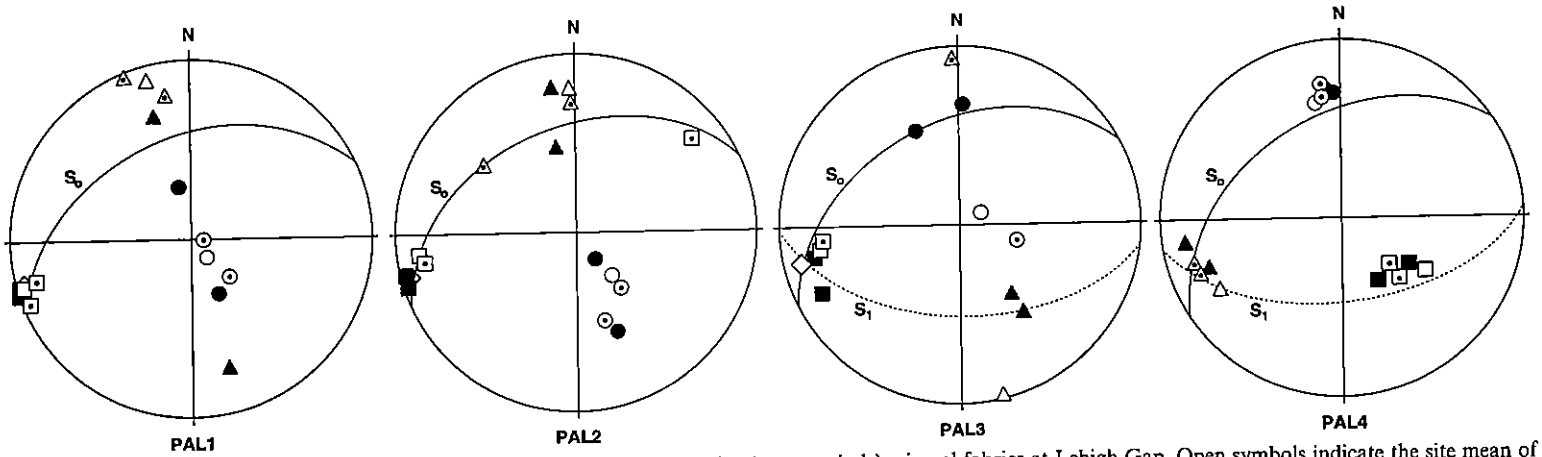

Fig. 6. Orientation of the principal axes of the chlorite (black symbols) and mica (grey symbols) mineral fabrics at Lehigh Gap. Open symbols indicate the site mean of low-field AMS and open symbols with dots show the paramagnetic component of individual samples from HFA. Maximum axes of the magnetic ellipsoids and minimum axes of the mineral fabric ellipsoids are shown by squares, intermediate axes by triangles, and minimum axes of the magnetic ellipsoids and maximum axes of the mineral fabric ellipsoids are shown by circles in this and subsequent figures. All axes are plotted on lower hemisphere, equal area stereograms. S_0 and S_1 are the bedding and cleavage planes, respectively.

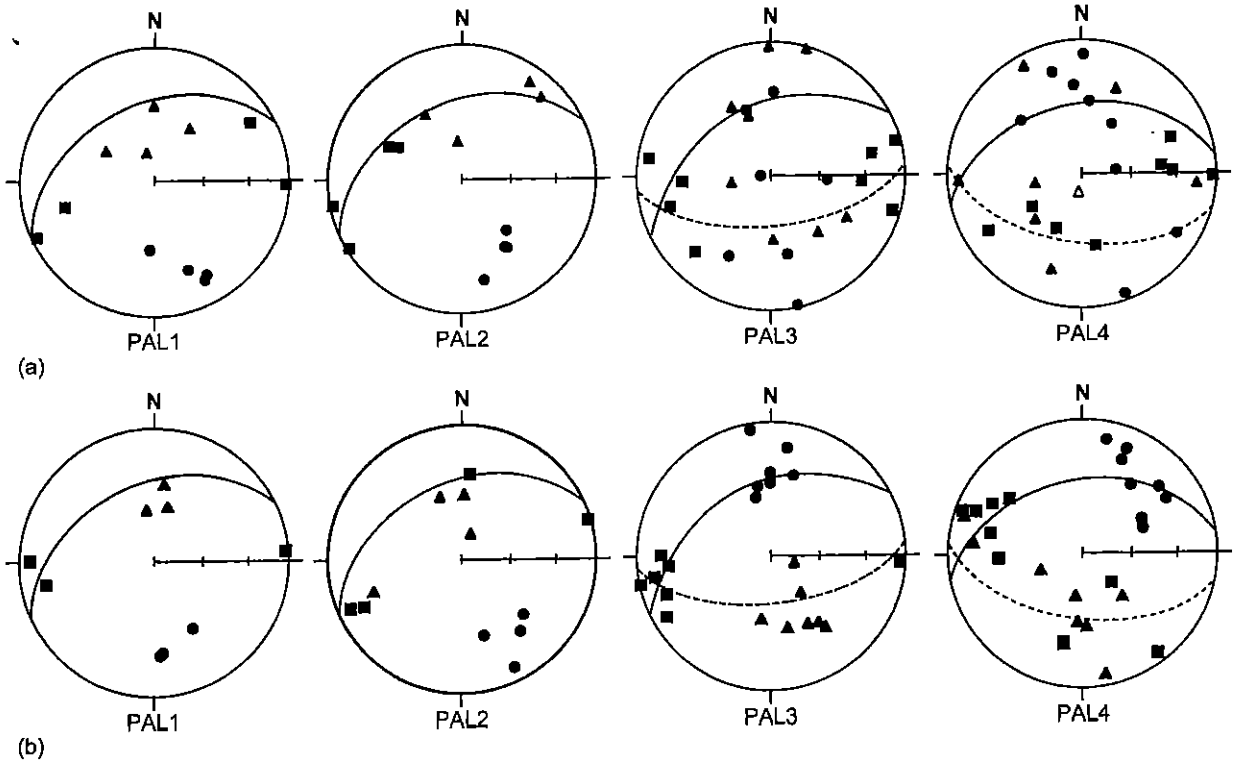

Fig. 7. Orientations of the principal axes of the AARM ellipsoids for (a) the low coercivity component (0.035 mT d.c. bias field, 0–30 mT a.c. field) and (b) the high coercivity component (0.5 mT d.c. bias field, 60–100 mT a.c. field). The bedding plane is shown with a solid line, cleavage plane with a dotted line.

Anisotropy of anhysteretic remanence

The two coercivity windows in which the ARM was acquired activate different grain-size populations of the magnetite, and possibly of pyrrhotite. The lower coercivity window will largely affect coarse detrital grains of magnetite. The higher coercivity window will activate finer grained magnetite and pyrrhotite.

The anisotropy of ARM (AARM) shows similar orientations in both coercivity windows for PAL1 and PAL2 (Fig. 7). The minimum axes are relatively well grouped and are closer to the bedding pole than the AMS fabric. This is again in agreement with the study of Housen & van der Pluijm (1991). At sites with a higher degree of deformation the fabrics in the two coercivity windows are no longer similar. The lower coercivity component is more poorly grouped, although there is still a loose grouping of k_1 axes close to the intersection lineation at PAL3 and an even looser grouping of k_3 axes close to the pole to cleavage at PAL4. The magnetic fabrics of the higher coercivity fractions at PAL3 and PAL4 exhibit the effects of cleavage flattening and intersection lineation.

Central Appalachian Fold and Thrust Belt, Pennsylvania

Electron microscopy and texture goniometry

The phyllosilicates at site MLM show alignment sub-parallel to the bedding plane and some minor and irregular kinking (Fig. 8a). The rocks do not contain much chlorite and the fabrics are very weak (Fig. 9). The minimum axes of chlorite and mica display weak clustering with some girdling of the mica axes. At site FAN, pencil structures are well developed. Both the chlorite and mica fabrics show weak girdling of the minimum axes caused by increased kinking (Fig. 9), which is also observed in the scanning electron microscope (SEM) data. The maximum axes for mica and chlorite group around the intersection lineation (Fig. 10); the minimum axes are only slightly offset from the bedding pole. A similar fabric can be observed at PLA.

The SEM data at site POR reveal a strong preferred orientation of the phyllosilicates parallel to the cleavage plane (Fig. 8b). Kinking is minor and new growth of grains occurs parallel to the cleavage plane. The minimum axes of chlorite and mica show clustered distributions with a strong point-maximum for mica and a weaker asymmetric maximum for chlorite, both normal to the cleavage plane (Fig. 9).

Anisotropy of magnetic susceptibility: low and high fields

Both low-field AMS, measured at 77 K, and HFA indicate that the susceptibility anisotropy is solely controlled by paramagnetic phases at all the sites. Bedding clearly controls the magnetic fabric at site MLM. There is a weak grouping of the k_1 and k_2 axes within the bedding plane (Fig. 10a). The AMS at site FAN is a classic 'pencil' fabric. The k_1 axes are well grouped along the intersection lineation and the k_2 and k_3 axes are spread out in a girdle. PLA also shows a pencil fabric, but there is a preferential clustering of k_3

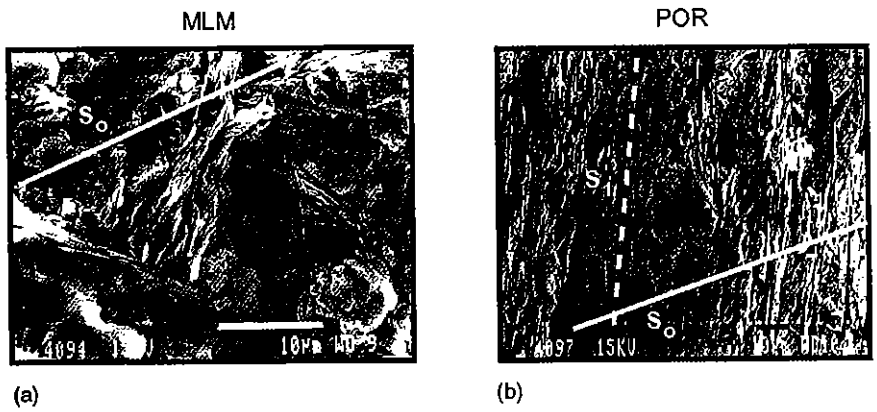

Fig. 8. SEM secondary electron images of the Appalachian fold and thrust belt showing kinking and microfolding at MLM and increased recrystallization parallel to the cleavage plane at POR. Scale bar represents **10 µm** in each image (white bar in (a), black bar in (b)). S_0 and S_1 are the traces of the bedding and cleavage planes, respectively.

POR1 chlorite
PLA1.1 chlorite
FAN chlorite
MLM

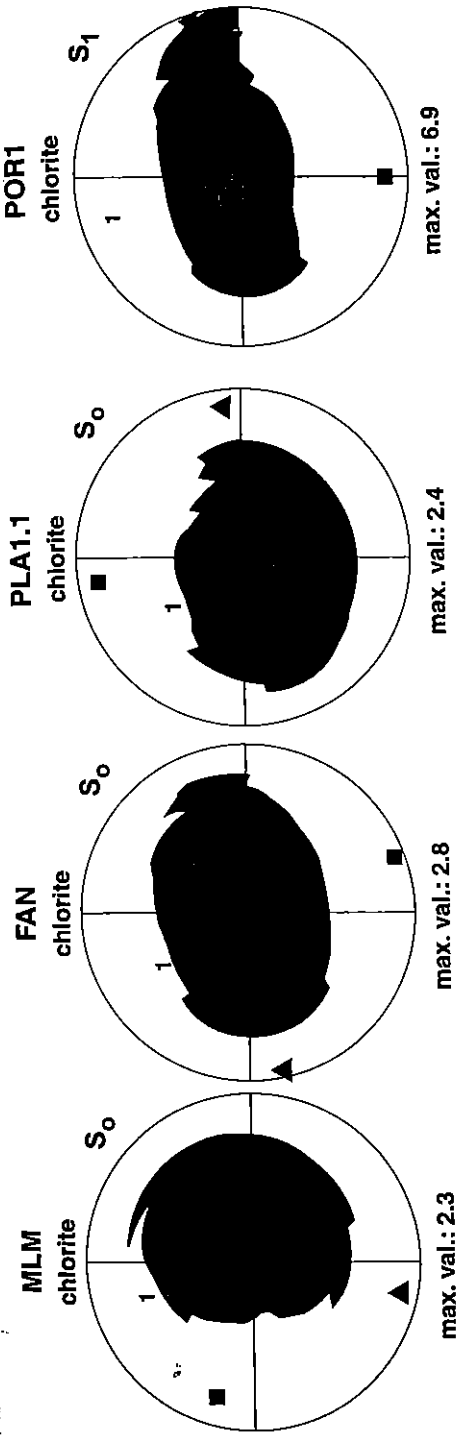

Fig. 9. X-ray texture goniometry pole figures of the Appalachian fold and thrust belt showing the transition of weak girdles to cluster distributions of the mica with increasing deformation. Chlorite pole figures are less well defined due to low chlorite content in these rocks. Contour interval is 0.5 m.r.d. at sites MLM, FAN and PLA, and 1.0 at POR. S_0 and S_1 are the bedding and cleavage planes, respectively.

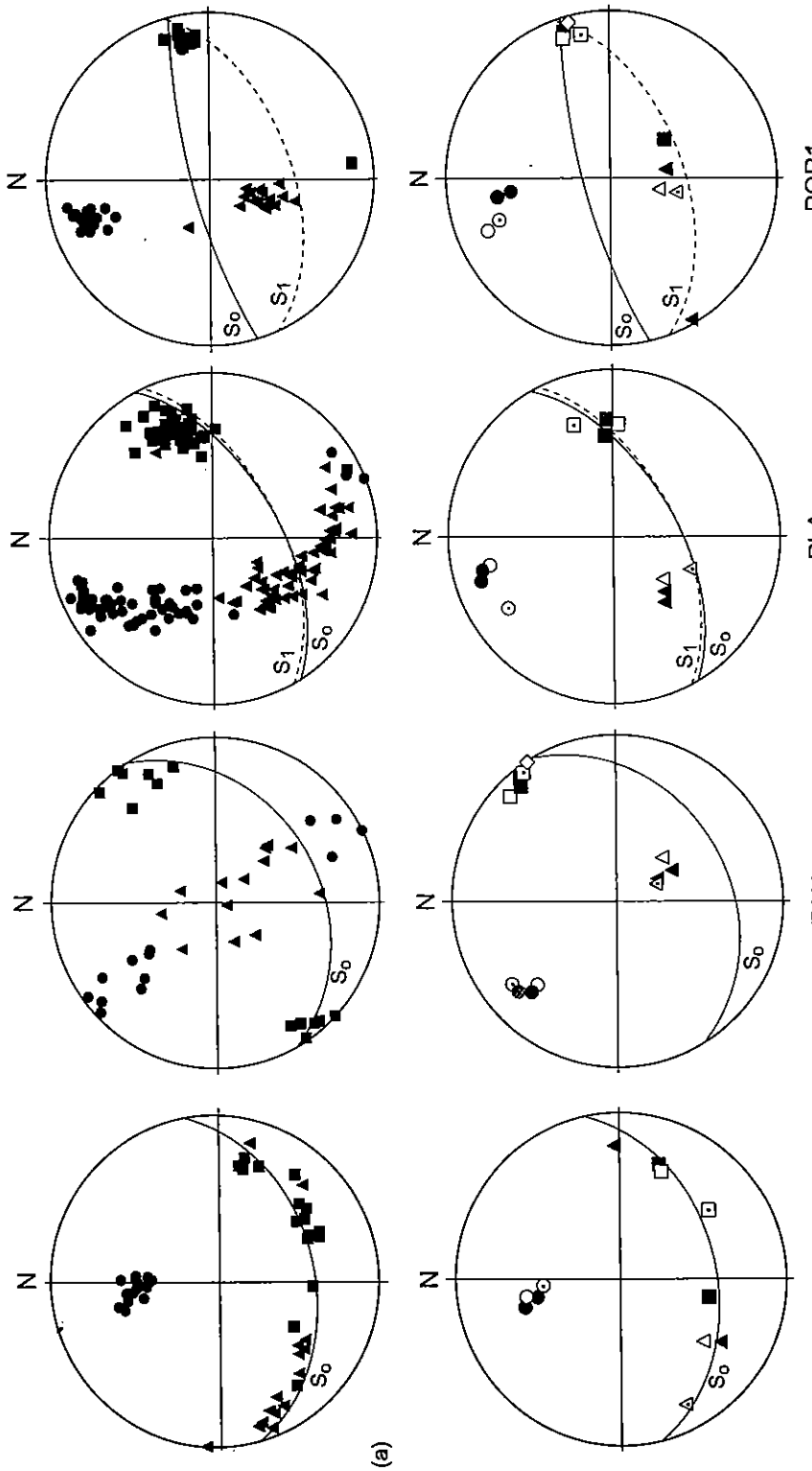

Fig. 10. (a) Orientations of the principal axes of the AMS ellipsoids of specimens from the fold belt. (b) Plots showing the chlorite (black symbols) and mica (grey symbols) mineral fabrics, the AMS from the sample used for the mineral fabric measurement (open symbols with dot), and the low-field site average (open symbols) for the sites across the fold belt. The bedding plane is shown with a solid line, cleavage plane with a dotted line and pencil lineation with a grey triangle. All axes are plotted on lower hemisphere, equal area stereograms. S_o and S_1 are the bedding and cleavage planes, respectively.

axes in the plane normal to the intersection lineation close to the pole to cleavage. A triaxial ellipsoid, in which all three axes are well grouped, characterizes the AMS at site POR, where k_3 is sub-parallel to the pole to cleavage and k_1 is sub-parallel to the observed lineation.

The orientations of the principal axes of the low-field AMS measured at 77 K and those of the HFA are very similar to the low-field AMS at room temperature. There is an excellent agreement of the principal axes of the AMS ellipsoid of the individual sample used for the texture goniometry measurement and the axes of the chlorite and mica fabric (Fig. 10b). This agreement supports the low-temperature and high-field results that attribute the anisotropy to paramagnetic phases. Since the chlorite and mica fabrics are similar, it is not possible to distinguish which is more important in defining the AMS.

Discussion

Graham (1966) described the evolution of the AMS ellipsoid shape that could be expected in sedimentary rocks that undergo a horizontal tectonic compaction. This pattern of fabric development was also reported by Kligfield *et al.* (1981) in Permian shales from the Alpes Maritimes, where they showed that the AMS was reflecting the strain that the rocks had undergone. Although both studies commented that the AMS development must be related to the orientation and anisotropy of the individual minerals, neither study provided a detailed analysis of the minerals responsible for the AMS. A combination of magnetic anisotropy, texture goniometry and SEM allows us to evaluate the development of magnetic and mineral fabric in more detail than these earlier works. The rocks at Lehigh Gap show the development of mineral and magnetic fabric over an outcrop scale. The shales show an original bedding compaction that is gradually overprinted by a horizontal tectonic shortening to form a slate. The tectonic shortening is first accommodated primarily by rotation and kinking of platy grains, as seen from the chlorite and mica fabrics. With increasing deformation neocrystallization of these minerals in the cleavage plane becomes a more dominant mechanism of grain reorientation. In SEM it can be observed that new grains are commonly smaller and aligned in cleavage lamellae, whereas detrital grains are found between the cleavage lamellae in the microlithons and are commonly larger and reoriented by mechanical rotation and kinking.

The low temperature and high field measurements have shown that the AMS is controlled by the paramagnetic minerals, and this accounts for the good agreement observed between the magnetic and mineral fabrics. At PAL1 and PAL2 the k_3 axes lie on the great circle between the t_3 axes of chlorite and mica, which suggests that both minerals are contributing to the AMS. At PAL4 the magnetic fabric is controlled by the cleavage, whereas the chlorite and mica still display girdled structures. This difference may be due to the fact that the texture goniometry was made on samples that had higher sand content than the samples used for the magnetic measurements, which indicates that the finer grain sizes take up the deformation more efficiently. The AARM results indicate that the orientation of the ferromagnetic minerals is controlled by bedding compaction at PAL1 and PAL2, and by cleavage at PAL3 and PAL4.

The remanent magnetic fabrics are better defined in the higher coercivity window than in the low coercivity window. This suggests that the finer grained magnetite and pyrrhotite particles are better aligned than the coarser, low coercivity grains. Most sedimentary rocks from the central Appalachian orogenic belt have undergone a pervasive remagnetization in the Late Permian. McCabe & Elmore (1989) and McCabe *et al.* (1989) found new growth of magnetite during deformation throughout the Appalachians, and attributed this to fluid flow during the orogeny. Stamatakos *et al.* (1996) interpreted the Late Permian remagnetization as taking place in a relatively short period of time more rapidly than the folding and thrusting propagated toward the foreland. Although we have no independent evidence for new growth of ferromagnetic phases, it is possible that the finer grains formed in the stress field during deformation, whereas the coarser grains underwent mechanical rotation together with the phyllosilicates. This leads to the development of a paramagnetic-related AMS that rotated passively during fold growth as predicted by Graham (1966).

An earlier study of the anisotropy of magnetic susceptibility and anhysteretic remanence at Lehigh Gap was made by Housen & van der Pluijm (1990; 1991). They found that the AMS (measured with a Sapphire Instrument (SI-2) susceptibility bridge in an applied field of 39 A/m (0.049 mT, at a frequency of 750–800 Hz) showed a sudden change from bedding-controlled fabric to cleavage-controlled fabrics at a distance from the contact with the Shawangunk sandstone corresponding to our site PAL3.

Fig. 10. (a) Orientations of the principal axes of the AMS ellipsoids of specimens from sites [illegible] (open symbols with dot), and the low-field site average (open symbols) symbols) mineral fabrics, the AMS from the sample used for the mineral fabric measurement (open symbols with dot), and the low-field site average (open symbols) for the sites across the fold belt. The bedding plane is shown with a solid line, cleavage plane with a dotted line and pencil lineation with a grey triangle. All axes are plotted on lower hemisphere, equal area stereograms. S_0 and S_1 are the bedding and cleavage planes, respectively.

This is in clear disagreement with our AMS results, which do not show an abrupt change but mirror the progressive deformation across the outcrop. The prolate AMS fabric, which we observe at PAL3, clearly reflects the observed mineral fabric. One difference between the two studies is that Housen & van der Pluijm (1990) took many small hand samples continuously along the outcrop. The disadvantage of this method is that only 2–4 specimens represent each site and the results may only reflect a very local fabric, rather than a more representative averaged fabric (cf. Lüneburg *et al.* 1999). In order to obtain statistically meaningful results we took a large number of samples at each site and located the sites across the outcrop so as to reveal the progressive variation.

Our AARM results are similar to those obtained by Housen & van der Pluijm (1991, their Fig. 4). They found that bedding clearly controls the AARM fabric in the first 55 m along the outcrop from the contact, which agrees with our results at PAL1 and PAL2. They reported some 'pencil fabrics' between 75 m and approximately 90 m and cleavage-controlled fabrics further along the outcrop, which is in agreement with our results at PAL3 and PAL4.

A similar pattern of progressive deformation is observed in the magnetic and mineral fabrics from the foreland of the fold-thrust belt to the hinterland. Sites close to the Appalachian Front have oblate magnetic fabrics. Some kinking of the phyllosilicate grains eventually leads to a grouping of the k_1 axes sub-parallel to the fold axes and in the direction of pencil structures. Pencil structure becomes better developed towards the east, and at approximately 70 km normal to the trend of the Allegheny Front the fabrics are prolate. Within 80 km of the Front an incipient cleavage is found in the finer grained lithologies. The Martinsburg Formation does not crop out again until further to the east in the hinterland, where a well-developed slaty cleavage is found. The POR locality shows evidence of significant recrystallization; pole figures exhibit high-density distributions of the phyllosilicate c axes that define triaxial AMS ellipsoids. These results imply a gradual progression of deformation across the Central Appalachian fold-thrust belt that is related to the gradual rotation and recrystallization of grains into the plane of the tectonic shortening.

Both transects, Lehigh Gap on the outcrop scale, and the Central Appalachian fold and thrust belt on the regional scale, show a gradual transition from shales to slates with progressive deformation. This transition is characterized by dominance of different deformation mechanisms, starting with mechanical reorientation of detrital grains by rotation and kinking and leading into new growth of grains parallel to the cleavage plane. The resulting microstructural patterns are reflected in the development of the mineral and magnetic fabric pole figure patterns, which range from cluster distributions, representing bedding (oblate fabric ellipsoids), to girdle distributions (prolate fabric ellipsoids) and again to cluster distributions representing cleavage. Both transects, although on different scales, exhibit the same characteristic patterns of progressive deformation and fabric development.

Conclusions

The development of magnetic fabric is shown to be closely related to the orientation of phyllosilicate grains on both an outcrop and regional scale in the Ordovician Martinsburg Formation in the Central Appalachian fold-thrust belt. The anisotropy of magnetic susceptibility in the rocks is carried exclusively by paramagnetic phases, and a good agreement is found between the mineral fabric of chlorite and mica and the AMS. At both Lehigh Gap and across Pennsylvania, the least deformed sites show bedding compaction with an intersection lineation sub-parallel to the trend of the major folds axes. This pattern develops into a true 'pencil' fabric, with a well-grouped intersection lineation, and later to a tectonic shortening. The development is gradual and is reflected in the orientation of the mineral grains and the magnetic anisotropy.

Financial support was provided by the Swiss National Science Foundation (NF Project: 20–28884.90) We thank G. Oertel, J. Stamatakos, K. Kodama and R. Nickelson for their helpful discussions. The constructive reviews of I. Abad, M. Sintubin and D. Tarling are gratefully acknowledged. We especially thank M. Sintubin for pointing out an error in an earlier figure. This is publication number 1320 of the Institute of Geophysics, ETH Zürich.

References

BALSLEY, J. R. & BUDDINGTON, A. F. 1960. Magnetic susceptibility and fabric of some Adirondack granites and orthogneisses. *American Journal of Science*, **258-A**, 6–20.

BECKER, J. K., SIEGESMUND, S. & JELSMA, H. A. 2000. The Chinamora batholith, Zimbabwe: structure and emplacement-related magnetic rock fabric. *Journal of Structural Geology*, **22**, 1837–1853.

CASEY, M. 1981. Numerical-analysis of x-ray texture data – an implementation in Fortran allowing triclinic or axial specimen symmetry and most crystal symmetries. *Tectonophysics*, **78**, 51–64.

CHEENEY, R. F. 1983. *Statistical Methods in Geology*. George Allen & Unwin, London, 169.

DAVIS, J. C. 1986. *Statistics and Data Analysis in Geology*, John Wiley & Sons, New York.

DE WALL, H., BESTMANN, M. & ULLEMEYER, K. 2000. Anisotropy of diamagnetic susceptibility in Thassos marble: A comparison between measured and modeled data. *Journal of Structural Geology*, **22**, 1761–1771.

ENGELDER, T. & ENGELDER, R. 1977. Fossil distortion and décollement tectonics of the Appalachian plateau. *Geology*, **5**, 457–460.

ENGELDER, T. & GEISER, P. 1979. The relationship between pencil cleavage and lateral shortening within the Devonian section of the Appalachian Plateau, New York. *Geology*, **7**, 460–464.

EPSTEIN, J. B. & EPSTEIN, A. G. 1969. Geology of the Valley and Ridge province between Delaware Water Gap and Lehigh Gap, Pennsylvania. *In*: SUBITZKY, S. (ed.) *Geology of Selected Areas in New Jersey and Eastern Pennsylvania, and Guidebook of Excursions*. Rutgers University Press, New Brunswick, 132–205.

EPSTEIN, A. G., EPSTEIN, J. B. & HARRIS, L. D. 1977. Conodont color alteration – an index to organic metamorphism. *U.S. Geological Survey Professional Papers*, **995**, 1–27.

FAILL, R. T. 1977. Fossil distortion, Valley and Ridge Province, Pennsylvania. *Geological Society of America Abstracts with Programs*, **9**, 262.

FAILL, R. T. 1997. A geologic history of the north-central Apppalachians, Part 1, Orogenesis from the Mesoproterozoic through the Taconic orogeny. *American Journal of Science*, **297**, 551–619.

FERRILL, D. A. & DUNNE, W. M. 1989. Cover deformation above a blind duplex: an example from West Virginia, U.S.A. *Journal of Structural Geology*, **11**, 421–431.

FULLER, M. D. 1963. Magnetic anisotropy and palaeomagnetism. *Journal of Geophysical Research*, **68**, 293–309.

GEISER, P. A. 1988. The role of kinematics in the construction and analysis of geological cross sections in deformed terranes. *In*: MITRA, G. & WOJTAL, S. (eds) *Geometries and Mechanisms of Thrusting*, Geological Society of America Special Paper **222**, 47–76.

GEISER, P. 1989. Day 5: Deformation fabrics and mechanisms of an 'autochthonous roof' duplex: The Valley and Ridge province of Pennsylvania and Maryland. *In*: Engelder, T. (ed.) *Structures of the Appalachian Foreland Fold-Thrust Belt, Field Trip Guidebook T166*. American Geophysical Union, Washington, D.C., 44–52.

GEISER, P. & ENGELDER, T. 1983. The distribution of layer parallel shortening fabrics in the Appalachian foreland of New York and Pennsylvania: Evidence for two non-coaxial phases of the Alleghanian orogeny. *Geological Society of America Memoir*, **158**, 161–175.

GIRDLER, R. W. 1961. Some preliminary measurements of anisotropy of magnetic susceptibility. *Geophysical Journal of the Royal Astronomical Society*, **5**, 197–206.

GRAHAM, J. W. 1954. Magnetic susceptibility anisotropy, an unexploited petrofabric element. *Geological Society of America Bulletin*, **65**, 1257–1258.

GRAHAM, J. W. 1966. Significance of magnetic anisotropy in Appalachian sedimentary rocks. *In*: Steinhart, J. S. & Smith, T. J. (eds) *The Earth Beneath the Continents*, Geophysical Monograph **10**. American Geophysical Union, Washington, 627–648.

GWINN, V. E. 1964. Thin skinned tectonics in the plateau and northwestern Valley and Ridge Provinces of the central Appalachians. *Geological Society of America Bulletin*, **75**, 863–900.

HATCHER, R. D., THOMAS, W. A., GEISER, P. A., SNOKE, A. W., MOSHER, S. & WILTSCHKO, D. V. 1989. Alleghanian orogen. *In*: HATCHER, R. D., THOMAS, W. A. & VIELE, G. W. (eds) *The Appalachian-Ouachita Orogen in the United States*. The Geological Society of America, Boulder, Colorado, The Geology of North America, **F-2**, 233–318.

HIRT, A. M., EVANS, K. F. & ENGELDER, T. 1995. Correlation between magnetic anisotropy and fabric for Devonian shales on the Appalachian Plateau. *Tectonophysics*, **247**, 121–132.

HO, N.-C., PEACOR, D. & VAN DER PLUIJM, B. 1995. Reorientation mechanisms of phyllosilicates in the mudstone-to-slate transition at Lehigh Gap, Pennsylvania. *Journal of Structural Geology*, **17**, 345–356.

HOLEYWELL, R. C. & TULLIS, T. E. 1975. Mineral reorientation and slaty cleavage in the Martinsburg Formation, Lehigh Gap, Pennsylvania. *Geological Society of America Bulletin*, **86**, 1296–1304.

HOUSEN, B. A. & VAN DER PLUIJM, B. A. 1990. Chlorite control of correlations between strain and anisotropy of magnetic susceptibility. *Physics of the Earth and Planetary Interiors*, **61**, 315–323.

HOUSEN, B. A. & VAN DER PLUIJM, B. A. 1991. Slaty cleavage development and magnetic anisotropy fabrics. *Journal of Geophysical Research*, **96**, 9937–9946.

IHMLÉ, P. F., HIRT, A. M., LOWRIE, W. & DIETRICH, D. 1989. Inverse magnetic fabric in deformed limestones of the Morcles nappe, Switzerland. *Geophysical Research Letters*, **16**, 1383–1386.

KLIGFIELD, R., OWENS, W. H. & LOWRIE, W. 1981. Magnetic susceptibility anisotropy, strain and progressive deformation in Permian sediments from the Maritime Alps (France). *Earth and Planetary Science Letters*, **55**, 181–189.

LOWRIE, W. 1990. Identification of ferromagnetic minerals in a rock by coercivity and unblocking temperature properties. *Geophysical Research Letters*, **17**, 159–162.

LÜNEBURG, C. M., LAMPERT, S. A., LEBIT, H. D., HIRT, A. M., CASEY, M. & LOWRIE, W. 1999. Magnetic anisotropy, rock fabrics and finite strain in deformed sediments of SW Sardinia (Italy). *Tectonophysics*, **307**, 51–74.

MARTÍN-HERNÁNDEZ, F. & HIRT, A. M. 2001. Separation of ferrimagnetic and paramagnetic anisotropies using a high-field torsion magnetometer. *Tectonophysics*, **337**, 209–222.

MCCABE, C. & ELMORE, D. 1989. The occurrence and origin of Late Paleozoic remagnetization in the sedimentary rocks of North America. *Reviews in Geophysics*, **27**, 471–494.

MCCABE, C., JACKSON, M. & ELLWOOD, B. B. 1985. Magnetic anisotropy in the Trenton limestone: results of a new technique, anisotropy of anhysteretic susceptibility. *Geophysical Research Letters*, **12**, 333–336.

MCCABE, C., JACKSON, M. & SAFFER, B. 1989. Regional patterns of magnetic authigenesis in the Appalachian basin: Implications for the mechanism of Late Paleozoic remagnetization. *Journal of Geophysical Research*, **94**, 10429–10443.

NICKELSEN, R. P. 1966. Fossil distribution and penetrative rock deformation in the Appalachian plateau. *Journal of Geology*, **74**, 924–931.

NICKELSEN, R. P. 1979. Sequence of structural stages of the Allegheny orogeny at the Bear Valley Strip Mine, Shamokin, Pennsylvania. *American Journal of Science*, **279**, 225–271.

OERTEL, G. 1983. The relationship of strain and preferred orientation of phyllosilicate grains in rocks: a review. *Tectonophysics*, **100**, 413–447.

RODGERS, J. 1963. Mechanics of Appalachian foreland folding in Pennsylvania and West Virginia. *American Association of Petroleum Geologists Bulletin*, **47**, 1527–1536.

SIDDANS, A. W. 1976. Deformed rocks and their textures. *Philosophical Transactions of the Royal Society of London*, **283**, 43- 54.

SIEGESMUND, S., ULLEMEYER, K. & DAHMS, M. 1995. Control of rock fabrics by mica preferred orientation: a quantitative approach. *Journal of Structural Geology*, **17**, 1601–1613.

STACEY, F. D., JOPLIN, G. & LINDSAY, J. 1960. Magnetic anisotropy and fabric of some foliated rocks from S.E. Australia. *Geofisica pura e applicata*, **47**, 30–40.

STAMATAKOS, J., HIRT, A. M. & LOWRIE, W. 1996. The age and timing of folding in the central Appalachians from paleomagnetic results. *Geological Society of America Bulletin*, **108**, 815–829.

WINTSCH, R. P., KVALE, C. M. & KISCH, H. J. 1991. Open-system, constant-volume development of slaty cleavage and strain-induced replacement reactions in the Martinsburg Formation, Lehigh Gap, Pennsylvania. *Geological Society of America Bulletin*, **103**, 916–927.

WRIGHT, T. O. & PLATT, L. B. 1982. Pressure dissolution and cleavage in the Martinsburg shale. *American Journal of Science*, **282**, 122–134.

WRIGHT, T. O., STEPHENS, G. C. & WRIGHT, E. K. 1979. A revised stratigraphy of the Martinsburg Formation of eastern Pennsylvania and paleogeographic consequence. *American Journal of Science*, **279**, 1176–1186.